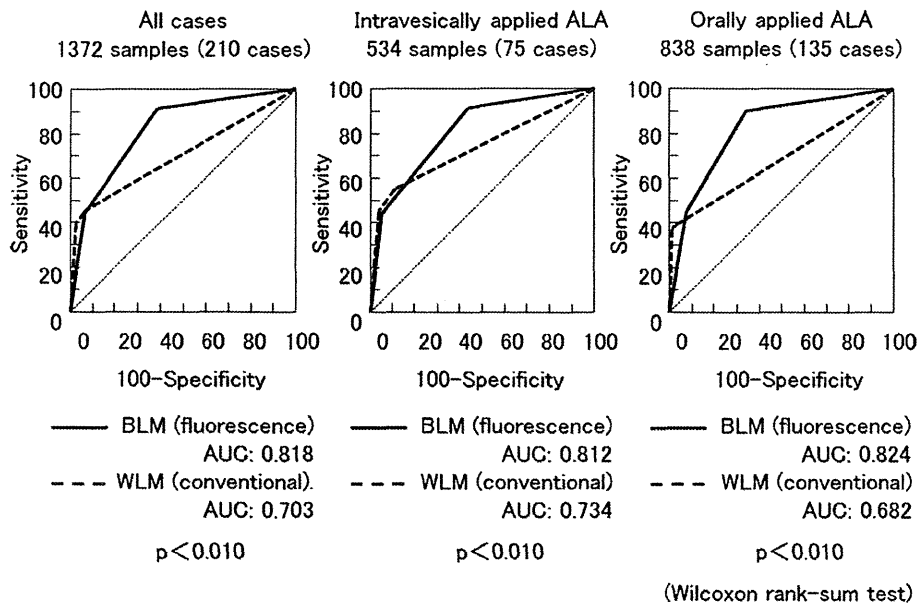

Figure 1. Diagnostic capability of photodynamic diagnosis (PDD) mediated by 5-aminolevulinic acid (ALA) (ALA-PDD) is defined by the area under the receiver operating characteristic curve (AUC). The AUC in blue light (fluorescence) mode (BLM) was more than that in white light (conventional) mode (WLM) in not only all PDD cases ($P < .01$) but also in PDD with intravesically applied ALA ($P < .01$) and PDD with orally applied ALA ($P < .01$).

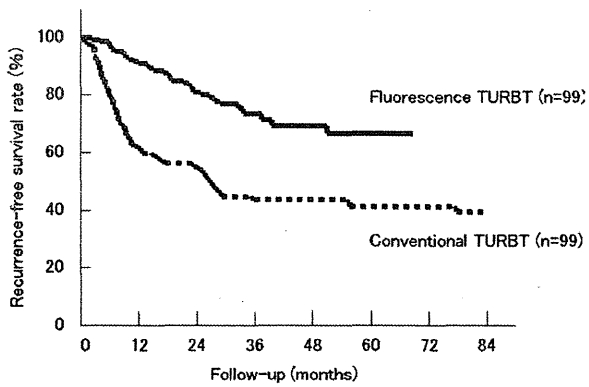

Figure 2. Recurrence-free survival in all cases is shown. Median follow-up period was 22.0 (range, 0.2-68.7) months in 99 patients who underwent transurethral resection of bladder tumor (TURBT) guided by photodynamic diagnosis mediated by 5-aminolevulinic acid. Thirty-three of 99 patients recurred, and recurrence-free survival rate was 86.9% (at 12 months), 74.7% (24 months), 69.7% (36 months), 67.7% (48 months), and 66.7% (60 months). Median follow-up period was 21.5 (range, 0.2-204.1) months in 99 patients who underwent conventional TURBT. Sixty of 99 patients recurred, and the recurrence-free survival rate was 58.6% (at 12 months), 49.5% (24 months), 41.4% (36 months), 41.4% (48 months), and 40.4% (60 months). There was a statistically significant difference in the recurrence-free survival rate between these 2 therapeutic groups ($P < .001$).

Moreover, multivariate analysis revealed that PDD-TURBT was the only independent factor that contributed to improving the intravesical recurrence rate (hazard ratio, 0.578; 95% confidence interval, 0.371-0.888; $P = .012$) (Table 7).

Adverse Events

Although no special precaution, such as liver support and light shielding, was implemented throughout PDD, there were mild and transient adverse events in conformity with the Common Terminology Criteria for Adverse Events version 3.0.[27] Urinary frequency and/or urgency occurred in 13 (17.3%) of 75 cases of PDD with intravesically applied ALA, photosensitivity reaction in 6 cases (4.4%), elevated level of AST and/or ALT in 4 cases (3.0%), and nausea and/or vomiting in 4 of 135 cases (3.0%) of PDD with orally applied ALA.

DISCUSSION

ALA-PDD is a cancer diagnostic method by fluorescence navigation, which has been clinically recognized as an effective procedure to detect various cancers, such as brain tumor[33] and bladder cancer.[10-17] In particular, PDD with hexaminolevulinate, the hexyl ester derivative of 5-ALA for bladder cancer, has already been approved and

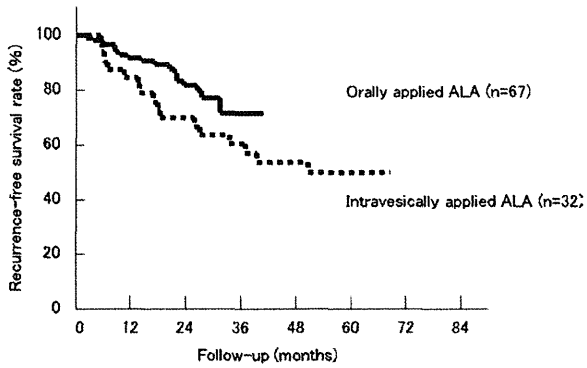

Figure 3. Recurrence-free survival stratified by 5-aminolevulinic acid (ALA) administration route is shown. Median follow-up period was 32.4 (range, 0.2-68.7) months in 32 patients who underwent transurethral resection of bladder tumor guided by photodynamic diagnosis mediated by ALA (PDD-TURBT) with intravesically applied ALA. Sixteen of 32 patients recurred, and recurrence-free survival rate was 84.4% (at 12 months), 68.8% (24 months), 59.4% (36 months), 53.1% (48 months), and 50.0% (60 months). Median follow-up period was 16.8 (range, 1.2-41.8) months in 70 patients who underwent PDD-TURBT with orally applied ALA. Nineteen of 67 patients recurred, and the recurrence-free survival rate was 86.6% (at 12 months), 76.1% (24 months), and 71.6% (36 months). There was no statistically significant difference in the recurrence-free survival rate between these 2 therapeutic groups ($P = .980$).

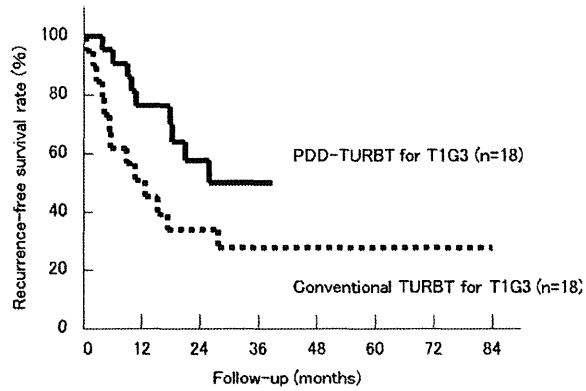

Figure 4. Recurrence-free survival is stratified by fluorescence transurethral resection of bladder tumor (TURBT) and conventional TURBT in T1G3. Median follow-up period was 18.1 (range, 3.7-38.8) months in 18 T1G3 patients who underwent TURBT guided by photodynamic diagnosis mediated by 5-aminolevulinic acid (PDD-TURBT). Nine of 18 patients recurred, and the recurrence-free survival rate was 72.2% (at 12 months), 55.6% (24 months), and 50.0% (36 months). Median follow-up period was 27.6 (range, 0.2-185.1) months in 18 T1G3 patients who underwent conventional TURBT. Thirteen of 18 patients recurred, and the recurrence-free survival rate was 47.3% (at 12 months), 33.3% (24 months), and 27.8% (36 months). There was no statistically significant difference in the recurrence-free survival rate between PDD-TURBT for T1G3 and conventional TURBT for T1G3 ($P = .062$). A deferred cystectomy because of recurrence and progression was performed in 1 case in the PDD-TURBT group and 2 cases in the conventional TURBT group. Median time to cystectomy was 7.9 months in the PDD-TURBT group, and 3.9 months and 10.4 months in the conventional TURBT group.

implemented as a legitimate medical practice in Europe and the United States, whereas in Japan, PDD with intravesically and orally applied ALA was performed for the first time in 2004,[29] and has just been approved and implemented as advanced medical technology in registered institutions by the Ministry of Health, Labor, and Welfare in 2010. In this study, we demonstrated the clinical effectiveness and safety of ALA-PDD and also of TURBT guided by ALA-PDD with a large population in Japan.

At transurethral biopsy, intravesical observation using ALA-PDD was useful in detecting CIS, avoiding an incorrect decision on adjuvant therapy. The diagnostic accuracy of ALA-PDD was first reported with a sensitivity of 100.0% and specificity of 68.5% in 68 cases of bladder cancer by Kriegmair et al[10] in 1994. Subsequently, many clinical trials of ALA-PDD have been performed, mainly in Europe. Hungerhuber et al[17] reported 1713 procedures of ALA-PDD with a sensitivity of 92.0% and specificity of 55.6% in 875 cases of bladder cancer, the largest number of ALA-PDD cases. Including these reports, a summary of previous reports revealed that the sensitivity of PDD (94.6%; range, 77.8%-100%) was significantly higher than the 76.0% (range, 67.5%-84.0%) sensitivity of conventional white light examination, whereas the specificity of PDD (59.0%; range, 33.0%-87.1%) was significantly lower than the 68.5% (range, 66.4%-78.0%) specificity of conventional white light examination.[10-17] In particular, the reports of flat lesions revealed that 34.2% (range, 14.9%-42.1%) of all lesions, 43.4%-57.0% of CIS, and 30.3%-44.0% of dysplasia could be detected by ALA-PDD, but not conventional white light

Table 7. Multivariate Analysis of All Cases

Factors	Hazard Ratio	95% Confidence Interval	*P*
EORTC recurrence score[32] (0, 1-4, 5-9, 10-17)	1.240	0.482-3.234	.657
BCG intravesical instillation	0.832	0.516-1.400	.475
PDD-TURBT	0.578	0.371-0.888	.012

Abbreviations: BCG, Bacillus Calmette-Guerin; EORTC, European Organization for Research and Treatment of Cancer; PDD-TURBT, transurethral resection of bladder tumor guided by photodynamic diagnosis.
Multivariate analysis revealed that the only independent factor contributing to improving prognosis was PDD-TURBT (hazard ratio, 0.578; 95% confidence interval, 0.371-0.888; $P = .012$).

examination.[15-17,34,35] The results of this study support the results of these clinical studies of ALA-PDD. The AUC in PDD with a sensitivity of 93.4% and specificity of 58.9% was significantly greater than that in conventional white light examination. Only PDD could detect 72.1% of flat lesions including dysplasia and CIS. Moreover, it was demonstrated that regardless of the ALA administration route, there was no significant difference in the diagnostic accuracy and ability of PDD in this study.

Causal lesions of intravesical recurrence are endoscopic invisible lesions. In TURBT, additional resection under ALA-PDD could avoid insufficient resection of tumors, reducing the rate of intravesical recurrence. The rate of residual tumor in PDD-TURBT with a median rate of 8.0% (0%-32.7%) was significantly reduced compared with conventional TURBT under white light, with a median rate of 37.0% (19.2%-53.1%) in the summary of previous reports.[14,18,21,36,37] Denzinger et al[22] made a comparative review of intravesical recurrence-free survival between 88 cases of PDD-TURBT and 103 cases of conventional TURBT, with 96 months as the follow-up duration. They reported that the intravesical recurrence-free survival of 90.9% (at 12 months after PDD-TURBT), 90.9% (24 months), 85.0% (48 months), 79.0% (72 months), and 71.0% (96 months) in PDD-TURBT was significantly greater than that in conventional TURBT of 78.6% (at 12 months after conventional TURBT), 69.9% (24 months), 60.7% (48 months), 54.0% (72 months), and 45.0% (96 months) ($P = .0003$). Moreover, it was demonstrated that PDD-TURBT was an independent prognostic factor for improving the intravesical recurrence rate, with a hazard ratio of 0.29 (95% confidence interval, 0.15-0.56; $P = .0002$) by multivariate analysis using the Cox proportional hazards model. The results of this study support the results of previous clinical studies of PDD-TURBT.[18-22] In this study, it was revealed that the intravesical recurrence-free survival was significantly greater than that in conventional TURBT at up to 60 months follow-up ($P < .001$). It was also revealed that PDD-TURBT was the only independent factor that contributed to improving the intravesical recurrence rate (hazard ratio, 0.578; 95% confidence interval, 0.371-0.888; $P = .012$) by multivariate analysis. Moreover, it was demonstrated that regardless of the ALA administration route, there was no significant difference in intravesical recurrence-free survival in this study.

In this study, only 18 cases of T1G3 were known to show highly aggressive behavior. PDD-TURBT for T1G3 had a greater tendency to reduce the intravesical recurrence rate, but with no statistically significant difference ($P = .062$) compared with conventional TURBT for T1G3 in this study population. However, more recently, the effectiveness of tumor control has been demonstrated in 77 cases of PDD-TURBT for T1G3[38]; therefore, more data compilation may show the usefulness of PDD-TURBT for T1G3 in improving recurrence-free survival and also avoiding deferred cystectomy because of tumor recurrence and progression.

Currently ALA and hexaminolevulinate have been approved as photosensitizers of PDD by authorities around the world. In Europe, ALA was approved under the trade name Gliolan as an optical imaging agent to enhance intraoperative detection of malignant glioma (World Health Organization grade III and IV) by the European Medicines Evaluation Agency.[9] Conversely, hexaminolevulinate was approved under the trade names Hexvix and Cysview as an optical imaging agent to enhance intraoperative detection of papillary bladder cancer by the European Medicines Evaluation Agency and the Food and Drug Administration in Europe and the United States, respectively.[9] More accumulation of biosynthesized protoporphyrin IX was revealed by administration of hexaminolevulinate compared with ALA by in vivo spectrophotometric measurement[39]; therefore, it was reported that hexaminolevulinate yielded higher fluorescence intensity and contrast between normal and malignant urothelium, with less photobleaching. In 2002, Dalton et al investigated the pharmacokinetics of ALA administered intravenously, orally, and intravesically, in which <1% of ALA was absorbed through the urinary bladder, and the cumulative ALA amount in urine was about 20,000× higher than that in plasma.[40] This finding indicates the low possibility of the occurrence of systemic adverse events induced by the intravesical administration of ALA, but does not demonstrate the usefulness for diagnosis compared with oral ALA administration, that is, differences in the fluorescence intensity between lesions and nonlesions (ie, contrast) and the fluorescence attenuation level with excitatory light irradiation (photobleaching) are parameters of diagnostic usefulness, and the diagnostic accuracy is based on these. We performed a clinical comparison of ALA administered intravesically and orally, and showed that the diagnostic accuracy of PDD was superior to that of white light examination excluding the predictive accuracy using intravesical ALA administration. In addition, there were no significant differences because of the variation in the route of administration (intravesical and oral ALA administrations) in diagnostic accuracy,

diagnostic performance, or recurrence-free survival. To pharmacologically demonstrate this subjective evaluation of clinical data and fluorescence intensity, we are planning to compare intravesical and oral ALA administrations with regard to tissue ALA and protoporphyrin IX levels in lesions and nonlesions, and the time course changes of these. Moreover, it was demonstrated in the retrospective series that currently, although PDD with ALA and hexaminolevulinate applied intravesically were demonstrated to be significantly superior to white light cystoscopy, there were no significant differences between ALA and hexaminolevulinate in clinical outcome such as residual tumor and recurrence-free survival.[26] Thus, in this study, we used ALA orally and intravesically to evaluate the clinical value in PDD and TURBT guided by ALA-PDD for bladder cancer. As described above, in this study, it was demonstrated that regardless of the ALA administration route, there was no significant difference in diagnostic accuracy, effectiveness of PDD, and recurrence-free survival, and all procedures were well tolerated by all patients without any severe adverse events. Although it is subjective, the intensity of ALA-induced fluorescence in PDD with orally applied ALA was higher than that in PDD with intravesically applied ALA. Moreover, PDD with orally applied ALA had less photobleaching. Hence, in the urological field, oral administration of ALA may be useful in PDD for malignancies other than bladder cancer. Further technical development of ALA-PDD is required to avoid photobleaching, improve diagnostic accuracy, and establish a standard intraoperative diagnostic system in the near future in Japan.

Conclusions

PDD with intravesically and also orally applied ALA is equally effective in detecting endoscopic invisible lesions such as dysplasia and carcinoma in situ, avoiding an incorrect decision on adjuvant therapy. In TURBT also, additional resection under ALA-PDD could avoid insufficient resection of tumors, reducing the rate of intravesical recurrence. It was suggested that regardless of the ALA administration route, ALA-PDD might be remarkably helpful in detection and intraoperative navigation programs.

FUNDING SOURCES

No specific funding was disclosed.

CONFLICT OF INTEREST DISCLOSURES

The authors made no disclosures.

REFERENCES

1. Jemal A, Siegel R, Xu J, et al. Cancer statistics 2010. *CA Cancer J Clin.* 2010;60:277-300.
2. Bray F, Sankila R, Ferlay J, et al. Estimates of cancer incidence and mortality in Europe in 1995. *Eur J Cancer.* 2002;38:99-166.
3. Matsuda T, Marugame T, Kamo K, et al. The Japan Cancer Surveillance Research Group. Cancer incidence and incidence rates in Japan in 2005: based on data from 12 population-based cancer registries in the Monitoring of Cancer Incidence in Japan (MCIJ) project. *Jpn J Clin Oncol.* 2011;41:139-147.
4. Lee R, Droller MJ. The natural history of bladder cancer. Implications for therapy. *Urol Clin North Am.* 2000;27:1-13, vii.
5. Navone NM, Polo CF, Frisardi AL, et al. Heme biosynthesis in human breast cancer—mimetic "in vitro" studies and some heme enzymic activity levels. *Int J Biochem.* 1990;22:1407-1411.
6. Fukuda H, Paredes S, Batlle AM. Tumour-localizing properties of porphyrins. In vivo studies using free and liposome encapsulated aminolevulinic acid. *Comp Biochem Physiol B.* 1992;102:433-436.
7. Steinbach P, Weingandt H, Baumgartner R, et al. Cellular fluorescence of the endogenous photosensitizer protoporphyrin IX following exposure to 5-aminolevulinic acid. *Photochem Photobiol.* 1995;62:887-895.
8. Baumgartner R, Fisslinger H, Jocham D, et al. A fluorescence imaging device for endoscopic detection of early stage cancer—instrumental and experimental studies. *Photochem Photobiol.* 1987;46:759-763.
9. Krammer B, Plaetzer K. ALA and its clinical impact, from bench to bedside. *Photochem Photobiol Sci.* 2008;7:283-289.
10. Kriegmair M, Baumgartner R, Knuechel R, et al. Fluorescence photodetection of neoplastic urothelial lesions following intravesical instillation of 5-aminolevulinic acid. *Urology.* 1994;44:836-841.
11. Kriegmair M, Baumgartner R, Knuchel R, et al. Detection of early bladder cancer by 5-aminolevulinic acid induced porphyrin fluorescence. *J Urol.* 1996;155:105-109.
12. Koenig F, McGovern FJ, Larne R, et al. Diagnosis of bladder carcinoma using protoporphyrin IX fluorescence induced by 5-aminolaevulinic acid. *BJU Int.* 1999;83:129-135.
13. Riedl CR, Plas E, Pfluger H. Fluorescence detection of bladder tumors with 5-amino-levulinic acid. *J Endourol.* 1999;13:755-759.
14. Filbeck T, Roessler W, Knuechel R, et al. Clinical results of the transurethral resection and evaluation of superficial bladder carcinomas by means of fluorescence diagnosis after intravesical instillation of 5-aminolevulinic acid. *J Endourol.* 1999;13:117-121.
15. Zaak D, Kriegmair M, Stepp H, et al. Endoscopic detection of transitional cell carcinoma with 5-aminolevulinic acid: results of 1012 fluorescence endoscopies. *Urology.* 2001;57:690-694.
16. Zaak D, Hungerhuber E, Schneede P, et al. Role of 5-aminolevulinic acid in the detection of urothelial premalignant lesions. *Cancer.* 2002;95:1234-1238.
17. Hungerhuber E, Stepp H, Kriegmair M, et al. Seven years' experience with 5-aminolevulinic acid in detection of transitional cell carcinoma of the bladder. *Urology.* 2007;69:260-264.
18. Filbeck T, Pichlmeier U, Knuechel R, et al. Clinically relevant improvement of recurrence-free survival with 5-aminolevulinic acid induced fluorescence diagnosis in patients with superficial bladder tumors. *J Urol.* 2002;168:67-71.

19. Filbeck T, Pichlmeier U, Knuechel R, et al. Clinically relevant reduction of recurrence of superficial bladder tumor with 5-aminolevulinic acid-induced fluorescence diagnosis. Results of a 5-year study. *Urologe A.* 2003;42:1366-1373.
20. Daniltchenko DI, Riedl CR, Sachs MD, et al. Long-term benefit of 5-aminolevulinic acid fluorescence assisted transurethral resection of superficial bladder cancer: 5-year results of a prospective randomized study. *J Urol.* 2005;174:2129-2133.
21. Babjuk M, Soukup V, Petrik R, et al. Fluorescence cystoscopy in the diagnostics and treatment of superficial urinary bladder tumors. *Cas Lek Cesk.* 2005;144:15-18.
22. Denzinger S, Burger M, Walter B, et al. Clinically relevant reduction in risk of recurrence of superficial bladder cancer using 5-aminolevulinic acid-induced fluorescence diagnosis: 8-year results of prospective randomized study. *Urology.* 2007;69:675-679.
23. Stenzl A, Burger M, Fradet Y, et al. Hexaminolevulinate guided fluorescence cystoscopy reduces recurrence in patients with nonmuscle invasive bladder cancer. *J Urol.* 2010;184:1907-1913.
24. Hermann GG, Mogensen K, Carlsson S, et al. Fluorescence-guided transurethral resection of bladder tumours reduces bladder tumour recurrence due to less residual tumour tissue in Ta/T1 patients: a randomized 2-centre study. *BJU Int.* [published online ahead of print March 17, 2011.]
25. Schumacher MC, Holmang S, Davidsson T, et al. Transurethral resection of non-muscle-invasive bladder transitional cell cancers with or without 5-aminolevulinic acid under visible and fluorescent light: results of a prospective, randomised, multicentre study. *Eur Urol.* 2010;57:293-299.
26. Burger M, Stief CG, Zaak D, et al. Hexaminolevulinate is equal to 5-aminolevulinic acid concerning residual tumor and recurrence rate following photodynamic diagnostic assisted transurethral resection of bladder tumors. *Urology.* 2009;74:1282-1286.
27. Common Terminology Criteria for Adverse Events version 3.0. *Inter J Clin Oncol.* 2004;9(suppl III):1-82.
28. Miyoshi N, Ogasawara T, Ogawa T, et al. An application of fluorescence analysis of metabolized protoporphyrin-IX (Pp-IX) in a tumor tissue administrated with 5-aminolevulinic acid (5-ALA). *J Jpn Soc Laser Med.* 2002;23:81-88.
29. Inoue K, Karashima T, Kamada M, et al. Clinical experience with intravesical instillations of 5-aminolevulinic acid (5-ALA) for the photodynamic diagnosis using fluorescence cystoscopy for bladder cancer. *Nippon Hinyokika Gakkai Zasshi.* 2006;97:719-729.
30. Inoue K, Kuno T, Fukuhara H, et al. Clinical experience with transurethral resection of bladder tumor (TUR-Bt) guided by photodynamic diagnosis (PDD). *Nippon Hinyokika Gakkai Zasshi.* 2009;100:661-670.
31. Japan Urological Association. General Rule for Clinical and Pathological Studies on Bladder Cancer. 3rd ed. Tokyo, Japan: Kanehara Publication; 2001.
32. Babjuk M, Oosterlinck W, Sylvester R, et al. EAU Guidelines on Non-Muscle-Invasive Urothelial Carcinoma of the Bladder, the 2011 update. *Eur Urol.* 2011;59:997-1008.
33. Utsuki S, Miyoshi N, Oka H, et al. Fluorescence-guided resection of metastatic brain tumors using a 5-aminolevulinic acid-induced protoporphyrin IX: pathological study. *Brain Tumor Pathol.* 2007;24:53-55.
34. Kriegmair M, Zaak D, Stepp H, et al. Transurethral resection and surveillance of bladder cancer supported by 5-aminolevulinic acid-induced fluorescence endoscopy. *Eur Urol.* 1999;36:386-392.
35. Filbeck T, Pichlmeier U, Knuechel R, et al. Do patients profit from 5-aminolevulinic acid-induced fluorescence diagnosis in transurethral resection of bladder carcinoma? *Urology.* 2002;60:1025-1028.
36. Riedl CR, Daniltchenko D, Koenig F, et al. Fluorescence endoscopy with 5-aminolevulinic acid reduces early recurrence rate in superficial bladder cancer. *J Urol.* 2001;165:1121-1123.
37. Kriegmair M, Zaak D, Rothenberger KH, et al. Transurethral resection for bladder cancer using 5-aminolevulinic acid induced fluorescence endoscopy versus white light endoscopy. *J Urol.* 2002;168:475-478.
38. Stanislaus P, Zaak D, Stadler T, et al. Photodynamic diagnosis in patients with T1G3 bladder cancer: influence on recurrence rate. *World J Urol.* 2010;28:407-411.
39. Marti A, Jichlinski P, Lange N, et al. Comparison of aminolevulinic acid and hexylester aminolevulinate induced protoporphyrin IX distribution in human bladder cancer. *J Urol.* 2003;170:428-432.
40. Dalton JT, Yates CR, Yin D, et al. Clinical pharmacokinetics of 5-aminolevulinic acid in healthy volunteers and patients at high risk for recurrent bladder cancer. *J Pharmacol Exp Ther.* 2002;301:507-512.

Clin Exp Metastasis (2012) 29:207–216
DOI 10.1007/s10585-011-9443-3

RESEARCH PAPER

Erlotinib prevents experimental metastases of human small cell lung cancer cells with no epidermal growth factor receptor expression

Adel Gomaa Mohammed Gabr · Hisatsugu Goto · Masaki Hanibuchi · Hirohisa Ogawa · Takuya Kuramoto · Minako Suzuki · Atsuro Saijo · Soji Kakiuchi · Van The Trung · Satoshi Sakaguchi · Yoichiro Moriya · Saburo Sone · Yasuhiko Nishioka

Received: 2 September 2011 / Accepted: 6 December 2011 / Published online: 15 December 2011

Abstract Epidermal growth factor receptor–tyrosine kinase inhibitors (EGFR–TKIs) show dramatic antitumor activity in a subset of patients with non-small cell lung cancer who have an active mutation in the epidermal growth factor receptor (EGFR) gene. On the other hand, some lung cancer patients with wild type EGFR also respond to EGFR–TKIs, suggesting that EGFR–TKIs have an effect on host cells as well as tumor cells. However, the effect of EGFR–TKIs on host microenvironments is largely unknown. A multiple organ metastasis model was previously established in natural killer cell-depleted severe combined immunodeficient mice using human lung cancer cells. This model was used to investigate the therapeutic efficacy of erlotinib, an EGFR–TKI, on multiple organ metastases induced by human small cell lung cancer cells (SBC-5 cells) that did not express EGFR. Although erlotinib did not have any effect on the proliferation of SBC-5 cells in vitro, it significantly suppressed bone and lung metastases in vivo, but not liver metastases. An immunohistochemical analysis revealed that, erlotinib significantly suppressed the number of osteoclasts in bone metastases, whereas no difference was seen in microvessel density. Moreover, erlotinib inhibited EGF-induced receptor activator of nuclear factor kappa-B expression in an osteoblastic cell line (MC3T3-E1 cells). These results strongly suggested that erlotinib prevented bone metastases by affecting host microenvironments irrespective of its direct effect on tumor cells.

Keywords Erlotinib · Bone metastasis · Lung cancer · Host microenvironment

A. G. M. Gabr · T. Kuramoto · S. Kakiuchi · V. T. Trung · S. Sone
Department of Medical Oncology, Institute of Health Biosciences, The University of Tokushima Gradate School, Tokushima, Japan

H. Goto · M. Hanibuchi · M. Suzuki · A. Saijo · S. Sakaguchi · S. Sone · Y. Nishioka (✉)
Department of Respiratory Medicine and Rheumatology, Institute of Health Biosciences, The University of Tokushima Graduate School, 3-18-15 Kuramoto-cho, Tokushima 770-8503, Japan
e-mail: yasuhiko@clin.med.tokushima-u.ac.jp

H. Ogawa
Department of Molecular and Environmental Pathology, Institute of Health Biosciences, The University of Tokushima Gradate School, Tokushima, Japan

Y. Moriya
Chugai Pharmaceutical Co., Ltd., Tokyo, Japan

Abbreviations

EGFR–TKI	Epidermal growth factor receptor–tyrosine kinase inhibitor
NSCLC	Non-small cell lung cancer
NK	Natural killer
SCID	Severe combined immunodeficient
SCLC	Small cell lung cancer
PTHrP	Parathyroid hormone-related protein
EGFR	Epidermal growth factor receptor
HUVECs	Human umbilical vein endothelial cells
IL	Interleukin
Ab	Antibody
VEGF	Vascular endothelial growth factor
MTT	3-(4,5-Dimethylthiazol-2-yl)-2,5-diphenyl tetrazolium
BMMSCs	Bone marrow mesenchymal stem cells
HGF	Hepatocyte growth factor

Introduction

Lung cancer is the major cause of malignancy-related death worldwide. The mortality rate is 80–90%, which makes this disease the leading cause of cancer-related death [1]. The high mortality of this disease is primarily due to the difficulty of early diagnosis and the highly metastatic potential. Approximately 70% of lung cancer patients have already developed metastases to multiple organs by the time of the diagnosis [2]. There is no curative therapy for the metastases, and clinical management is palliative in many cases. Therefore, it is crucial to prevent and treat lung cancer metastases.

Although the outcome of conventional chemotherapy for patients with advanced lung cancer is still unsatisfactory, recent studies have enabled the development of molecular targeting agents such as epidermal growth factor receptor–tyrosine kinase inhibitors (EGFR–TKIs). Treatment with the reversible EGFR–TKIs (gefitinib and erlotinib) results in dramatic antitumor activity in a subset of patients with non-small cell lung cancer (NSCLC). Approximately 75% of patients with epidermal growth factor receptor (EGFR) mutations respond to EGFR–TKIs [3, 4]. The inhibition of EGFR tyrosine kinase results in the induction of substantial apoptosis in these tumor cells because lung cancer cells that have an active mutation in the EGFR gene become addicted to the EGFR signaling pathway for their growth. This mechanism allows EGFR–TKIs to exert anti-tumor activity in NSCLC patients with an active mutation in the EGFR gene.

However, it is noteworthy that an objective response of about 10% is also achieved with erlotinib treatment in NSCLC patients with wild type EGFR [5]. These clinical observations indicate that EGFR–TKIs might have other mechanisms of action in addition to their direct effect on tumor cells. Normanno et al. [6] demonstrated that gefitinib inhibits the recruitment of osteoclasts in bone lesions, by affecting the ability of bone marrow stromal cells to induce osteoclast differentiation and activation. Moreover, Cerniglia et al. [7] reported that erlotinib treatment of tumor-bearing mice alters vessel morphology and decreases vessel permeability in tumor xenografts. These observations suggest that EGFR–TKIs have the potential to modulate and affect host cells, but their effect on the host microenvironment in different organs with cancer metastases is largely unknown.

The establishment of clinically relevant experimental metastasis models is crucial to understand the pathogenesis of lung cancer and its relationship to host microenvironment. A reproducible model of multiple organ metastases by human lung cancer cells was previously established in natural killer (NK) cell-depleted severe combined immunodeficient (SCID) mice [8, 9]. This model was used to elucidate the mechanisms of interactions of metastatic lung cancer cells with host organ microenvironment and the heterogeneity in organ microenvironments on the metastases of human lung cancer [10–14].

The present study sought to elucidate the action of EGFR–TKIs on host microenvironments in organs with lung cancer metastases. The study investigated the therapeutic efficacy of erlotinib, an EGFR–TKI, on multiple organ metastases induced by SBC-5 human small cell lung cancer (SCLC) cells that did not express EGFR in NK cell-depleted SCID mice.

Materials and methods

Cell cultures

The human SCLC cell line, SBC-5 [15] was kindly provided by Drs. M. Tanimoto and K. Kiura (Okayama University, Okayama, Japan). The PC-9 human adenocarcinoma cell line was purchased from the American Type Culture Collection (Manassas, VA). SBC-5 cells were maintained in Eagle's MEM (Nissui Pharmaceutical Co., Tokyo, Japan) supplemented with 10% heat-inactivated fetal bovine serum (FBS, GIBCO, Grand Island, NY), penicillin (100 U/ml), and streptomycin (50 μg/ml). PC-9 cells were maintained in RPMI1640 (Nissui Pharmaceutical Co., Tokyo, Japan) supplemented with 10% heat-inactivated FBS, penicillin and streptomycin. The MC3T3-E1 murine osteoblastic cell line subclone 4 was kindly provided by Chugai Pharmaceutical Co., Ltd. (Tokyo, Japan). MC3T3-E1 cells were maintained as preosteoblasts in α-MEM growth medium supplemented with 10% FBS, penicillin and streptomycin. The growth medium was supplemented with L-ascorbic acid (50 μg/ml) to induce differentiation, and the cells were cultured for 7 days [16]. All cell lines were incubated at 37°C in a humidified atmosphere of 5% CO_2 in air.

Reagents

An anti-mouse interleukin (IL)-2 receptor β chain monoclonal antibody (Ab), TM-β1 (IgG2b), was kindly provided by Drs. M. Miyasaka and T. Tanaka (Osaka University, Osaka, Japan) [17]. Recombinant murine EGF was purchased from Invitrogen (Carlsbad, CA). None of these materials contained endotoxins, as determined by the limulus amebocyte assay (Seikagaku Kogyo, Tokyo, Japan: minimum detection level, 0.1 ng/ml).

In vitro cell proliferation and migration assay

Cell proliferation was determined using the 3-(4,5-dimethylthiazol-2-yl)-2,5-diphenyl tetrazolium (MTT) dye reduction method [18]. The human lung cancer cells

(2×10^3 cells/100 μl) were plated into each well of a 96-well plate, and incubated overnight. Various concentrations of erlotinib were added and the cells incubated for 72 h. Fifty microliters of stock MTT solution (2 mg/ml; Sigma-Aldrich, St. Louis, MO) was added to all wells, and the cells were then further incubated for 2 h at 37°C. The media containing MTT solution were removed, and 100 μl of DMSO (Sigma-Aldrich, St. Louis, MO) was added. The absorbance was measured with an MTP-32 Microplate Reader (Corona Electric, Ibaragi, Japan) at test and reference wavelengths of 550 and 630 nm, respectively. Cell migration was determined using double chamber method. RPMI-1640 medium (0.75 ml) containing 10% FBS was applied to the lower chamber as chemoattractant, and SBC-5 cells (5×10^4) in 0.5 ml of serum-free RPMI-1640 medium were seeded in inner chamber (8 μm-pore, BD Labware, Franklin Lakes, NJ) with the presence of 0, 0.01, 0.1 or 1 μM erlotinib, and incubated for 19 h at 37°C. After incubation, cells remaining on the upper side of the insert were removed, and the cells that migrated to the lower surface of the insert were counted in four different random fields at 100× magnification. Each treatment was performed in triplicate.

Animals

Male, 6 to 8-week-old S EB-17/Icr-scid mice were obtained from Clea Japan (Osaka, Japan) and maintained under specific pathogen-free conditions throughout the experiment. The experimental protocol was reviewed and approved by the animal care and use committee of The University of Tokushima, and were performed according to their guidelines.

Experimental metastasis with SBC-5 cells and the effect of erlotinib

NK cells were depleted in SCID mice to facilitate the metastasis of human lung cancer cell lines. TM-β1 Ab (0.3 mg/mouse) was injected i.p. into SCID mice 2 days before tumor inoculation [8]. Tumor cells were harvested and washed with Ca^{2+}- and Mg^{2+}-free phosphate buffered saline (Nissui Pharmaceutical Co., Tokyo, Japan). Cell viability was determined by a trypan blue exclusion test and only single cell suspensions of >90% viability were used. SBC-5 cells (1×10^6 cells/0.3 ml/mouse) were inoculated into the lateral tail vein of unanesthetized SCID mice pretreated with TM-β1 Ab on day 0. Oral administration of erlotinib (10 or 30 mg/kg) was performed once daily from day 7 to 28. Vehicle was administered to the control group. Mice were anesthetized and humanely sacrificed on day 29 by cutting the subclavian artery, and all major organs were removed. Whole body X-ray photographs (Fuji Film, Tokyo, Japan) of tumor-bearing mice were taken just before sacrifice and bone metastases were independently evaluated on X-ray photographs by two authors [9]. The lungs were fixed in Bouin's solution (Sigma-Aldrich, St. Louis, MO) for 24 h. The number of metastatic foci on the lungs, liver were counted macroscopically.

Immunohistochemistry

The hind limbs of the mice were taken and fixed in 10% formalin. The bone specimens were decalcified in 10% EDTA solution for 1 week and then embedded in paraffin. The paraffin-embedded tissue samples were cut into 3-μm sections and picked up on slides. Tartrate-resistant acid phosphatase (TRAP) staining was performed using a Sigma Diagnostics Acid Phosphatase Kit (Sigma Diagnostics, St. Louis, MO) for the detection of osteoclasts. The number of TRAP-positive osteoclasts at the tumor-bone interface in each slide was counted under a microscope in five random fields at 200× magnification. Formalin fixed, paraffin embedded sections were stained with anti-mouse CD31 Ab (Santa Cruz Biotechnology, Santa Cruz, CA). CD31 positive microvessels were counted from five independent fields at 200× magnification of each section. The sections were also stained with H&E for routine histologic examination.

Western blot analysis

The cells were seeded at 1×10^6 cells/dish in corresponding differentiation conditions to assess the effects of exogenous stimuli on the activation of the EGFR in MC3T3-E1 cells. Differentiated cells were cultured for 24 h in medium containing 1% FBS, and subsequently treated with recombinant EGF for 10 min in the absence or presence of various concentrations of erlotinib. Cells were lysed in M-PER (Pierce, Rockford, IL) containing phosphatase inhibitor cocktail and proteinase inhibitor cocktail (Roche Diagnostics, Indianapolis, IN), and the protein concentration was determined using a protein assay kit (Bio-Rad, Hercules, CA). Aliquots of 400 μg of total protein were immunoprecipitated with the anti-mouse EGFR Ab (Cell signaling, Danvers, MA), and the immune complexes were recovered with Protein G-Sepharose beads (GE Healthcare, Buckinghamshire, UK). Proteins were separated by SDS-PAGE (Invitrogen, Carlsbad CA) and then transferred to PVDF membranes (Atto, Tokyo, Japan). Washed membranes were incubated with Blocking One (Nacalai Tesque, Kyoto, Japan) for 1 h at room temperature, then incubated 1 h at room temperature with anti-phosphotyrosine Ab (1:1,000 dilution, cell signaling) or anti-EGFR Ab (1:2,00 dilution, cell signaling). The membranes were

incubated for 30 min at room temperature with species-specific horseradish peroxidase conjugated secondary antibodies, and the immunoreactive bands were visualized using an enhanced chemiluminescent substrate (Pierce, Rockford, IL).

Reverse transcription polymerase chain reaction

MC3T3-E1 cells were seeded at 1×10^6 cells/well in 6-well plates in the corresponding differentiation conditions. The differentiated cells were treated with recombinant EGF in the absence or presence of indicated dose of erlotinib for 48 h. Total cellular RNA was isolated by using RNeasy Mini kit (Qiagen, Valencia, CA) according to the manufacturer's protocols. RNA (0.5–2.0 μg) was reverse transcribed using a TaqMan® RNA-to-CT™ 2-Step kit (Applied biosystems, Foster City, CA). Messenger The expression of receptor activator of nuclear factor kappa-B ligand (RANKL), osteoprotegerin (OPG) and EGFR mRNA were measured by real-time polymerase chain reaction (PCR) using Assay on Demand Taqman Gene expression primers and probes (Applied biosystems). PCR reaction conditions were those recommended by the manufacturer. Fluorescence signals were monitored after each PCR cycle with an ABI Prism 7700 sequence detection system (Applied Biosystems). C_T values (cycle number where fluorescence exceeded a fixed threshold) were obtained for each target probe and normalized with the corresponding C_T values for the internal control (mouse $\beta 2$ microglobulin). The RNA levels were expressed as relative units.

Statistical analysis

The Mann–Whitney *U* test was used to evaluate the differences in the numbers of metastases into multiple organs (bone, liver, and lung) between the erlotinib-treated groups and the control (vehicle treated group), and to evaluate the differences in immunohistochemistry. The differences in in vitro experiments were analyzed by Student's *t* test (two-tailed). A P value of <0.05 was considered to be significant in all experiments.

Results

Erlotinib did not affect the proliferation and migration of human SCLC, SBC-5 cells in vitro

We have previously reported that SBC-5 cells do not express EGFR [12]. In this study, we first examined the effect of erlotinib on in vitro proliferation and migration of SBC-5 cells. As shown in Fig. 1a, clinically relevant doses

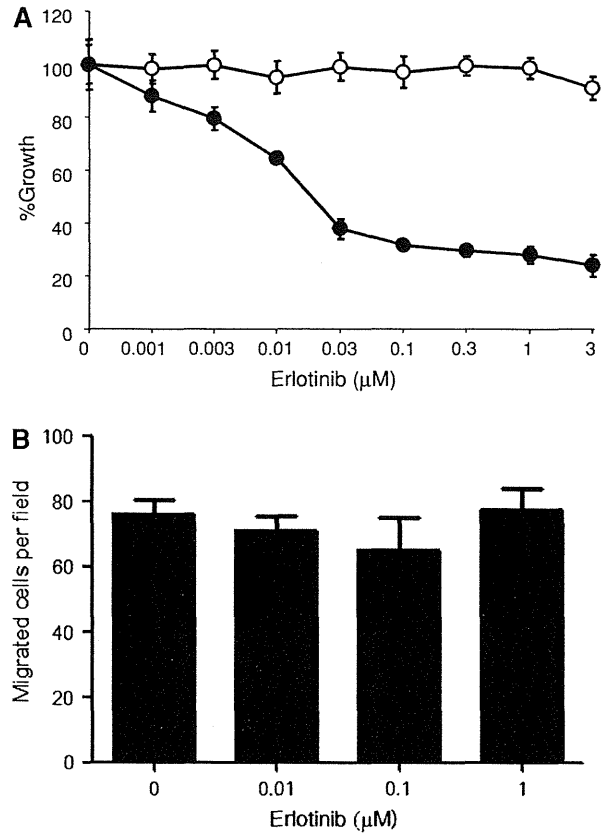

Fig. 1 Effect of erlotinib on the proliferation and migration of human SCLC, SBC-5 cells in vitro. **a** SBC-5 cells (1×10^3 cells/well; *open circles*) or PC-9 cells (1×10^3 cells/well; *closed circles*) were plated into each well of a 96-well plate and incubated overnight. Various concentrations of erlotinib were added and the cells were incubated for 72 h. Cell growth was determined by MTT assay as described in "Materials and methods" section. *Bars* show SDs of the means of triplicate cultures. Data are representative of five independent experiments. **b** Cell migration of SBC-5 cells was assessed as described in "Materials and methods" section. *Bars* show SDs of the means of triplicate cultures. Data are representative of two independent experiments

(3 μM or less) of erlotinib [19] had no effect on the proliferation of SBC-5 cells. On the contrary, erlotinib significantly inhibited the proliferation of PC-9 cells, which harbor a deletion mutation on exon 19 of the EGFR gene, in a dose-dependent fashion (Fig. 1a), consistent with a previous report [20]. Cell migration of SBC-5 cells was also not affected by erlotinib treatment (Fig. 1b).

Treatment with erlotinib inhibited bone and lung metastases by SBC-5 cells in NK cell-depleted SCID mice

A multiple organ metastasis model with SBC-5 cells was established in SCID mice depleted of NK cells [9]. Intravenously inoculated SBC-5 cells (1×10^6/mouse)

developed metastatic colonies in the lungs, liver, and bones (osteolytic metastasis) of NK cell-depleted SCID mice. This model was used to assess the therapeutic efficacy of erlotinib. Oral administration of erlotinib (30 mg/kg) from day 7 to 28 significantly inhibited the formation of osteolytic bone metastases (Fig. 2). Interestingly, treatment with erlotinib also inhibited distant metastases in the lungs, although it had no effect on liver metastases (Table 1). Erlotinib treatment was well tolerated and no obvious adverse events, such as body weight loss, were observed even in the 30 mg/kg group (data not shown). These in vivo results suggested that erlotinib prevented distant metastases by affecting the host microenvironments because erlotinib had no direct effect on the proliferation of SBC-5 cells in vitro.

Effect of erlotinib on tumor angiogenesis

Guillamo et al. [21] reported that EGFR–TKI (gefitinib) inhibits angiogenesis in a mouse experimental glioma model. Moreover, Riedel et al. [22] reported that addition of conditioned medium from EGFR antisense-treated tumor cells decreases endothelial cell migration and proliferation. These findings suggested that the prevention of SBC-5-induced metastasis formation by erlotinib could be due to the inhibition of angiogenesis. However, immunohistochemical staining with CD31 revealed no significant difference in the microvessel density in the lung, bone, and liver (Fig. 3). The effect of erlotinib on the proliferation of human umbilical vein endothelial cells (HUVECs) was also evaluated in vitro. Up to 3 μM of erlotinib did not

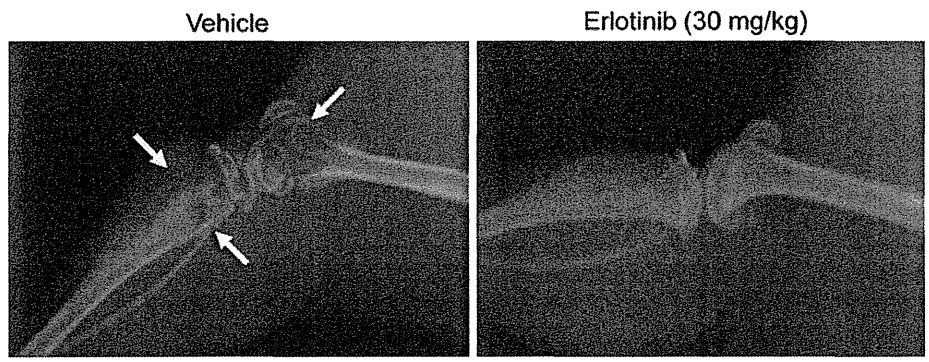

Fig. 2 Therapeutic efficacy of erlotinib against osteolytic bone metastases produced by human SCLC, SBC-5 cells. SBC-5 cells (1×10^6 cells/mouse) were inoculated into the tail vein of NK cell-depleted SCID mice. Oral administration of erlotinib was performed as described in "Materials and methods" section. Mice were sacrificed and bone metastases were determined radiographically on day 29. The representative pictures of vehicle- and erlotinib-treated mice are shown. The *arrows* indicate osteolytic bone metastases

Table 1 Effect of erlotinib on multiple organ metastasis produced by SBC-5 cells

Treatment	Bone			Liver					Lung				
	Number of metastasis			Weight (g)		Number of metastasis			Weight (g)		Number of metastasis		
	Inc.	Med.	Range	Med.	Range	Inc.	Med.	Range	Med.	Range	Inc.	Med.	Range
Experiment 1													
Vehicle	6/6	6	5–7	1.6	1.3–1.9	6/6	39	25–80	0.3	0.3–0.4	6/6	38	30–55
10 mg/kg	5/5	5	3–6	1.4	1.0–1.7	5/5	23	12–35	0.3	0.2–0.5	5/5	20	8–30
30 mg/kg	5/5	3*	2–5	2.0	1.8–3.4	5/5	26	2–38	0.3	0.3–0.4	5/5	15*	6–35
Experiment 2													
Vehicle	6/6	9	7–11	1.8	1.6–2.4	6/6	60	20–150	0.22	0.24–0.41	6/6	14	5–20
10 mg/kg	6/6	8	5–11	1.6	1.3–1.8	6/6	31	10–50	0.24	0.29–0.4	6/6	10	9–11
30 mg/kg	6/6	4*	2–6	1.5	1.8–3.3	6/6	24	12–40	0.21	0.3–0.4	6/6	7*	2–11

SBC-5 cells (1×10^6 cells/mouse) were inoculated i.v. into NK cell-depleted SCID mice on day 0. Erlotinib (or vehicle) was given orally from day 7 to 28 after tumor cell inoculation. The metastatic profile was evaluated on day 29. Mann–Whitney *U* test was used to determine the significance of differences

Inc. incidence, *Med.* median

* Statistically significant difference compared with vehicle-treated group ($P < 0.05$)

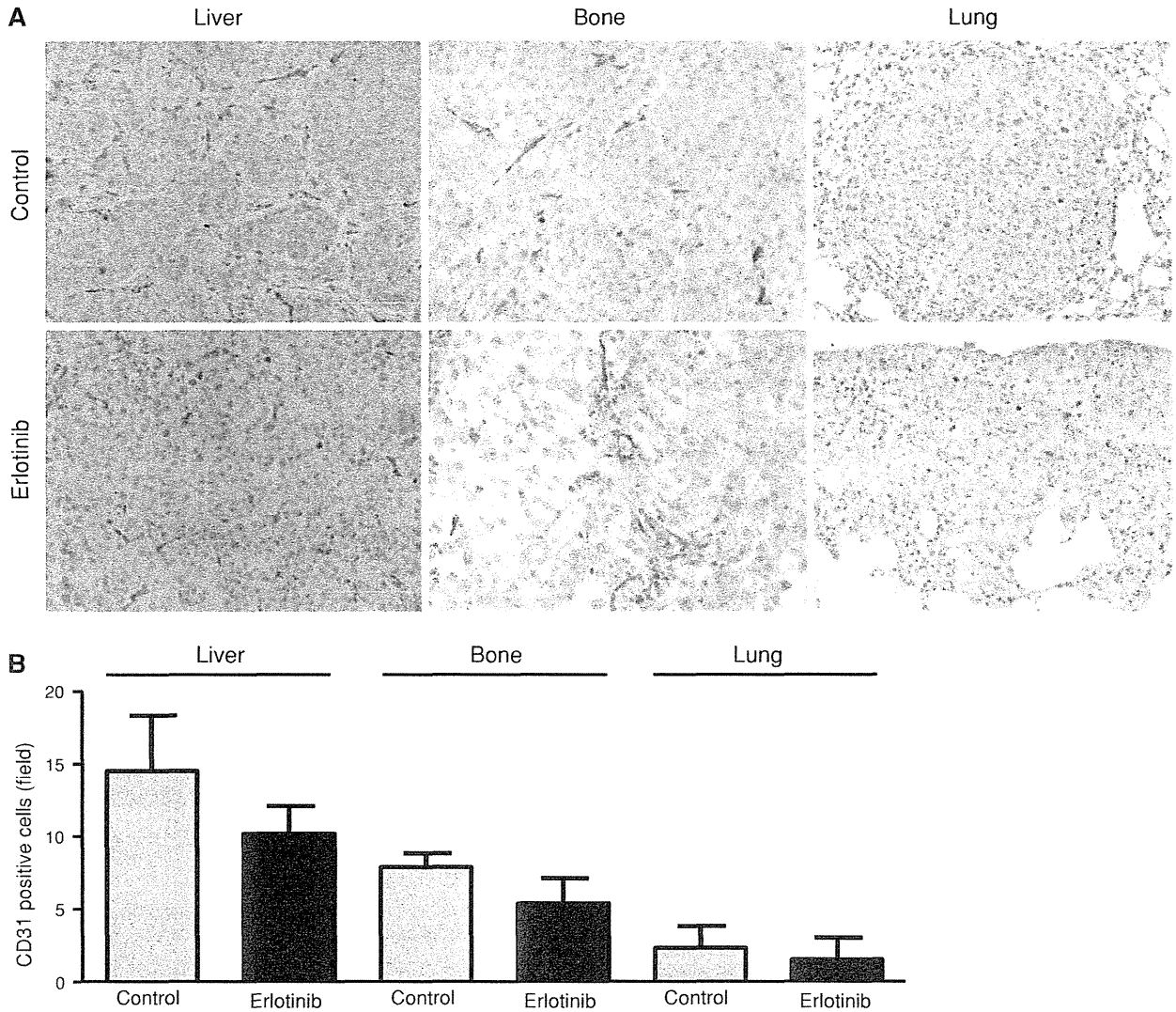

Fig. 3 Effect of erlotinib on tumor angiogenesis. SBC-5 cells (1×10^6 cells/mouse) were inoculated into the tail vein of NK cell-depleted SCID mice. Oral administration of erlotinib was performed as described in "**Materials and methods**" section. Each organ was collected on day 29, paraffin embedded, and sections were subjected to immunohistochemical staining of CD31. **a** Representative pictures of immunohistochemical staining are shown (magnification, ×200). **b** CD31 positive microvessels were counted from five independent fields of each section. *Bars* show SEM of the means for five mice per group

affect the proliferation of HUVECs irrespective of the stimulation with recombinant human vascular endothelial growth factor (VEGF) (data not shown).

Erlotinib reduced the number of osteoclast in bone metastasis lesion

A previous study demonstrated the importance of osteoclasts in bone metastasis development by SBC-5 cells [9, 10]. Immunohistochemical staining (TRAP staining) was performed to evaluate the number of osteoclasts in metastatic bone lesions. Figure 4 demonstrates that erlotinib treatment significantly reduced the number of osteoclasts (TRAP positive cells) in metastatic bone lesions.

Erlotinib inhibited EGF-induced RANKL expression in osteoblastic cell line MC3T3-E1 cells

RANKL is one of the key molecules responsible for the formation of osteolytic bone metastasis in various types of cancer [23]. RANKL expressed by osteoblasts activates osteoclasts by binding to its receptor (RANK). The fact that the number of osteoclasts in bone metastasis lesions decreased after erlotinib treatment suggested that erlotinib

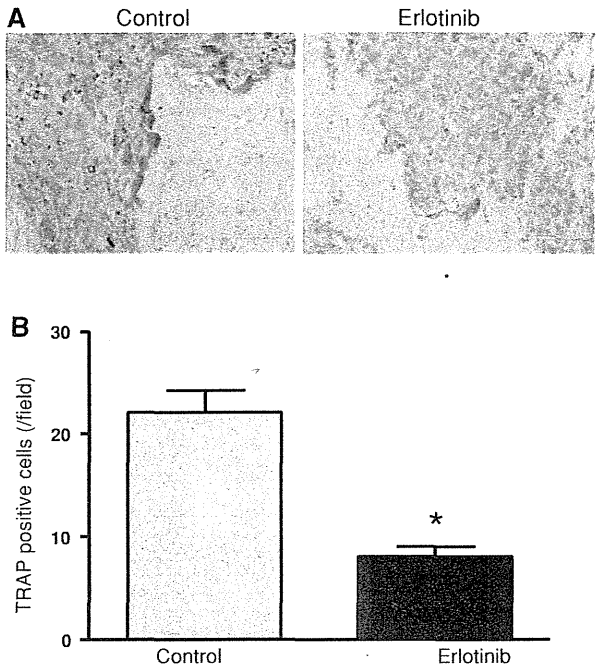

Fig. 4 The effect of erlotinib on osteoclast recruitment in metastatic bone lesion. SBC-5 cells (1×10^6 cells/mouse) were inoculated into the tail vein of NK cell-depleted SCID mice. Oral administration of erlotinib was performed as described in "Materials and methods" section. Metastatic bone lesions were collected on day 29, and sections were subjected to TRAP staining to evaluate osteoclast recruitment. **a** Representative pictures of TRAP staining of bone are shown (magnification, ×200). TRAP positive cells were stained in *purple*. **b** The number of osteoclasts (TRAP positive cells) was counted from five independent fields of each section. *Bars* show the SEM of the means for five mice per group. $*P < 0.01$

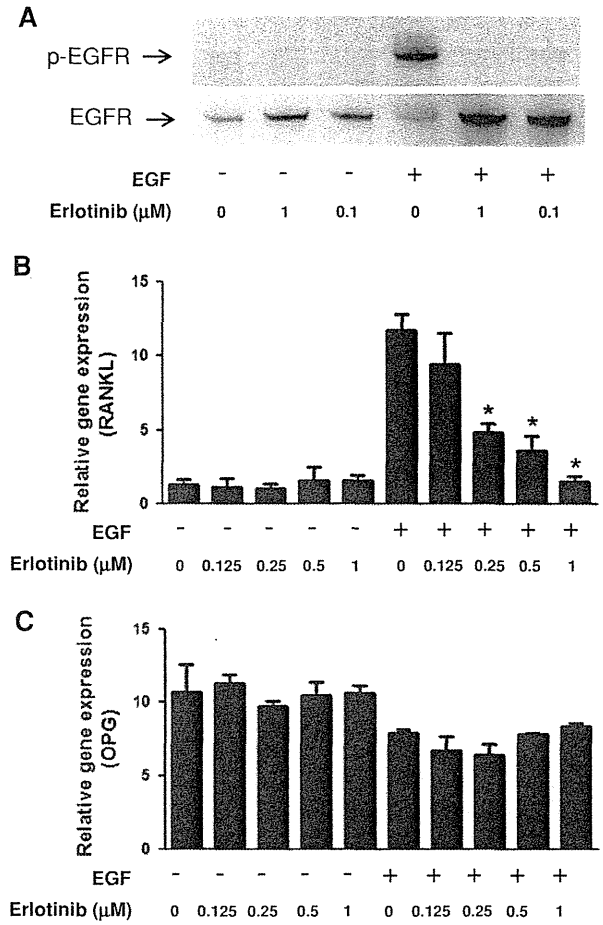

Fig. 5 The effect of erlotinib on osteoblastic cell line MC3T3-E1 cells. Murine osteoblastic cell line MC3T3-E1 cells were differentiated into the mature state as described in "Materials and methods" section. **a** Differentiated cells were treated with EGF (10 ng/ml) for 10 min in the presence or absence of erlotinib. Expression of EGFR and phosphorylated EGFR (p-EGFR) was detected by western blotting. **b**, **c** Differentiated MC3T3-E1 cells were treated with EGF (10 ng/ml) in the presence or absence of various concentrations of erlotinib for 48 h. The cells were harvested, and the expression of **b** RANKL and **c** OPG was detected by RT-PCR. *Bars* show the SEM of the means of triplicate cultures. $*P < 0.01$

suppresses osteoclast differentiation and activation by inhibiting the RANK–RANKL axis. The expression of EGFR in the osteoblastic cell line MC3T3-E1 cells was evaluated, since EGFR is reported to be expressed in osteoblasts but not in osteoclasts [16]. Figure 5a shows that MC3T3-E1 cells did express EGFR, and its phosphorylation was induced by EGF treatment. The inhibition of EGFR phosphorylation by erlotinib was also confirmed. EGF induced RANKL expression in MC3T3-E1 cells, and the expression was significantly suppressed by erlotinib in a dose dependent manner (Fig. 5b). Interestingly, the expression of OPG, the decoy receptor for RANKL, was not affected by either EGF or erlotinib treatment (Fig. 5c).

Discussion

The present study demonstrated that erlotinib significantly suppressed bone and lung metastases, but not liver metastases, by SBC-5 cells that did not express EGFR. These findings suggest the importance of the host microenvironment in the treatment of lung cancer with erlotinib. The formation of distant metastasis involves several sequential steps, including tumor growth in the primary site, invasion into blood vessels, arrest in the capillaries, extravasation, invasion and growth in target organs [24, 25]. Molecular interactions between cancer cells and their microenvironments play important roles that allow the cancer cells to survive at metastatic sites, [24–27]. Therefore, the efficacy of therapeutic agents against cancer metastases depends on their mechanisms of action on tumor cells as well as the host microenvironments.

There is accumulating evidence that the EGFR ligand-EGFR axis plays a role in in bone biology and pathology. The expression and functionality of EGFR has been clearly

demonstrated in bone marrow mesenchymal stem cells (BMMSCs) [6, 28], and osteoblasts themselves differentiate from mesenchymal stem cells [29]. In addition, EGFR ligands, such as EGF and amphiregulin, stimulate the proliferation of BMMSCs and osteoblasts [30–32], suggesting that EGFR ligands are mitogens for BMMSCs and osteoblasts. EGFR signaling also indirectly affects osteoclast formation, although osteoclasts do not express functional EGFR [16]. The role of EGFR in osteoclast formation suggests that the balance of RANKL and OPG (the decoy receptor for RANKL), which are expressed by osteoblasts, is associated with differentiation. The current study showed that the expression of RANKL, not OPG, in osteoblasts was stimulated by EGF, and this might enhance osteoclast activation via the RANK/RANKL axis. This result is supported by previous study reported by Furugaki et al. [33]. Using mouse osteolytic bone invasion model, they showed that the lung cancer cells induced RANKL expression of osteoblasts, and erlotinib inhibited the tumor-induced osteolytic invasion by suppressing osteoclast activation through inhibiting osteolytic factor production including RANKL. The importance of the balance of RANKL and OPG is also supported by Zhu et al. [16]. They demonstrated that EGFR ligands stimulate osteoclast formation by inhibiting the expression of OPG by osteoblasts, although RANKL expression was not affected. This difference might be due to differences in the experimental conditions and EGFR ligands. The importance of osteoclasts and osteoblasts on the development of bone metastases [16, 34] suggests that EGFR–TKIs prevent bone metastasis formation by inhibiting the activation of osteoclasts and osteoblasts in addition to their direct effect on tumor cells.

Current evidence also suggests the association of EGFR signaling with primary bone tumor and bone metastasis formation. EGFR upregulation is observed in osteosarcomas and osteosarcoma cell lines [35], bone and soft tissue tumors [36]. Furthermore, EGFR is overexpressed in a variety of tumors metastasizing to bone. Prostate cancer is the best studied example. EGFR expression correlates with prostate cancer relapse and progression to androgen independence [37] and the blockade of EGFR signaling by PKI166, an EGFR–TKI, inhibits prostate cancer growth in the bones of nude mice [38]. Gefitinib, an EGFR–TKI, inhibits the recruitment of osteoclasts in metastatic bone lesions from breast cancer by affecting the ability of bone marrow stromal cells to induce osteoclast differentiation and activation [6]. Moreover, gefitinib administered to breast cancer patients (phase II trial) with bone metastasis significantly attenuates and relieves bone pain [6]. Collectively, EGFR–TKIs might thus have the potential to regulate the progression of bone metastases by acting on not only tumor cells but also host microenvironments, thus suggesting the importance of targeting the EGFR signaling blockade in the prevention of bone metastases.

The current study found that erlotinib prevented distant metastases in the bone and the lungs but not in the liver, thus suggesting that organ heterogeneity is important in the pathogenesis of lung cancer metastasis. Organ heterogeneity in the therapeutic response is frequently observed in experimental xenograft models as well as in the clinical setting. Macrophage colony-stimulating factor gene transduction into human squamous cell lung carcinoma, RERF-LC-AI cells significantly suppresses experimental metastases in the liver but not the kidneys [13]. Treatment with, bevacizumab, an anti-human VEGF Ab, inhibits distant metastases of human ACC-LC-319/bone2 adenocarcinoma cells in the bone and the liver but not the lungs [14]. These observations imply that the heterogeneity of organ microenvironments affects the progression of lung cancer metastases.

The current experiments did not reveal why erlotinib failed to inhibit liver metastases, but one plausible explanation is that hepatocyte growth factor (HGF), which is produced by stromal cells in the liver as well as other organs, might be responsible for organ heterogeneity in the therapeutic response observed in this study. HGF acts as a potent mitogen for endothelial cells and binds to receptors expressed on endothelial cells, thus stimulating angiogenesis [39]. Yano et al. [40] demonstrated that HGF induces gefitinib resistance of lung adenocarcinoma cells with EGFR-activating mutations by restoring the phosphatidylinositol 3-kinase/Akt signaling pathway via phosphorylation of MET. These reports suggest that the microenvironment in the liver may not be favorable for EGFR–TKIs to exert antitumor activity. The current in vivo results also showed that erlotinib had therapeutic efficacy against lung metastases. Pulmonary vascular destabilization in the premetastatic phase promotes the extravasation of breast cancer cells and facilitates lung metastasis, indicating that vascular normalization might lead to the suppression of lung metastasis [41]. In addition, Cerniglia et al. [7] reported that erlotinib treatment with tumor-bearing mice alters vessel morphology and decreases vessel permeability in tumor xenografts, resulting in vascular normalization. Although erlotinib failed to show an inhibitory effect on tumor angiogenesis in this study, these findings indicate that EGFR–TKIs might prevent lung metastases by decreasing vessel permeability and preventing extravasation of tumor cells. Baker et al. [42] have previously reported that the EGFR expression of host cells such as endothelial cells is conditioned by tumor microenvironment. Thus, there is a possibility that EGFR expression status of SBC-5 cells might also be regulated by host organ microenvironment, although it is still unclear that EGFR expression of cancer cells is conditioned by

tumor microenvironment. Further studies are warranted to elucidate the mechanism of organ heterogeneity in the therapeutic response by erlotinib.

In summary, the current study demonstrated that erlotinib significantly suppressed bone and lung metastases by SBC-5 cells which did not express EGFR, while it had no inhibitory effect on the proliferation of SBC-5 cells in vitro. Even though the precise mechanisms remain uncertain, these results strongly suggested that erlotinib prevented distant metastasis formation by affecting host microenvironments irrespective of its direct effect on tumor cells. Erlotinib might therefore be a promising therapeutic candidate for the inhibition of distant metastases.

Acknowledgments This work was supported in part by a Grant-in-aid for Cancer Research from the Ministry of Education, Science, Sports and Culture of Japan, and Ministry of Health and Welfare of Japan.

References

1. Jemal A, Siegel R, Ward E, Hao Y, Xu J, Thun MJ (2009) Cancer statistics 2009. CA Cancer J Clin 59:225–249
2. Sone S, Yano S (2007) Molecular pathogenesis and its therapeutic modalities of lung cancer metastasis to bone. Cancer Metastasis Rev 26:685–689
3. Jackman DM, Yeap BY, Sequist LV, Lindeman N, Holmes AJ, Joshi VA, Bell DW, Huberman MS, Halmos B, Rabin MS, Haber DA, Lynch TJ et al (2006) Exon 19 deletion mutations of epidermal growth factor receptor are associated with prolonged survival in non-small cell lung cancer patients treated with gefitinib or erlotinib. Clin Cancer Res 12:3908–3914
4. Riely GJ, Pao W, Pham D, Li AR, Rizvi N, Venkatraman ES, Zakowski MF, Kris MG, Ladanyi M, Miller VA (2006) Clinical course of patients with non-small cell lung cancer and epidermal growth factor receptor exon 19 and exon 21 mutations treated with gefitinib or erlotinib. Clin Cancer Res 12:839–844
5. Mitsudomi T, Yatabe Y (2007) Mutations of the epidermal growth factor receptor gene and related genes as determinants of epidermal growth factor receptor tyrosine kinase inhibitors sensitivity in lung cancer. Cancer Sci 98:1817–1824
6. Normanno N, De Luca A, Aldinucci D, Maiello MR, Mancino M, D'Antonio A, De Filippi R, Pinto A (2005) Gefitinib inhibits the ability of human bone marrow stromal cells to induce osteoclast differentiation: implications for the pathogenesis and treatment of bone metastasis. Endocr Relat Cancer 12:471–482
7. Cerniglia GJ, Pore N, Tsai JH, Schultz S, Mick R, Choe R, Xing X, Durduran T, Yodh AG, Evans SM, Koch CJ, Hahn SM, Quon H, Sehgal CM, Lee WM, Maity A (2009) Epidermal growth factor receptor inhibition modulates the microenvironment by vascular normalization to improve chemotherapy and radiotherapy efficacy. PLoS ONE 4:6539–6549
8. Yano S, Nishioka Y, Izumi K, Tsuruo T, Tanaka T, Miyasaka M, Sone S (1996) Novel metastasis model of human lung cancer in SCID mice depleted of NK cells. Int J Cancer 67:211–217
9. Miki T, Yano S, Hanibuchi M, Sone S (2000) Bone metastasis model with multiorgan dissemination of human small-cell lung cancer (SBC-5) cells in natural killer cell-depleted SCID mice. Oncol Res 12:209–217
10. Miki T, Yano S, Hanibuchi M, Kanematsu T, Muguruma H, Sone S (2004) Parathyroid hormone-related protein (PTHrP) is responsible for production of bone metastasis, but not visceral metastasis, by human small cell lung cancer SBC-5 cells in natural killer cell-depleted SCID mice. Int J Cancer 108:511–515
11. Yano S, Zhang H, Hanibuchi M, Miki T, Goto H, Uehara H, Sone S (2003) Combined therapy with a new bisphosphonate, minodronate (YM529), and chemotherapy for multiple organ metastases of small cell lung cancer cells in severe combined immunodeficient mice. Clin Cancer Res 9:5380–5385
12. Yano S, Muguruma H, Matsumori Y, Goto H, Nakataki E, Edakuni N, Tomimoto H, Kakiuchi S, Yamamoto A, Uehara H, Ryan A, Sone S (2005) Antitumor vascular strategy for controlling experimental metastatic spread of human small cell lung cancer cells with ZD6474 in natural killer cell-depleted severe combined immunodeficiency mice. Clin Cancer Res 11:8789–8798
13. Yano S, Nishioka Y, Nokihara H, Sone S (1997) Macrophage colony-stimulating factor gene transduction into human lung cancer cells differentially regulates metastasis formations in various organ microenvironments of natural killer cell-depleted SCID mice. Cancer Res 57:784–790
14. Otsuka S, Hanibuchi M, Ikuta K, Yano S, Goto H, Ogino H, Yamada T, Kakiuchi S, Nishioka Y, Takahashi T, Sone S (2009) A bone metastasis model with osteolytic and osteoblastic properties of human lung cancer ACC-LC-319/bone2 in natural killer cell-depleted severe combined immunodeficient mice. Oncol Res 17:581–591
15. Kiura K, Watarai S, Shibayama T, Ohnoshi T, Kimura I, Yasuda T (1993) Inhibitory effects of cholera toxin on in vitro growth of human lung cancer cell lines. Anticancer Drug Des 8:417–428
16. Zhu J, Jia X, Xiao G, Kang Y, Partridge NC, Qin L (2007) EGF-like ligands stimulate osteoclastogenesis by regulating expression of osteoclast regulatory factors by osteoblasts: implications for osteolytic bone metastases. J Biol Chem 282:26656–26664
17. Tanaka T, Kitamura F, Nagasaka Y, Kuida K, Suwa H, Miyasaka M (1993) Selective long-term elimination of natural killer cells in vivo by an anti-interleukin 2 receptor β chain monoclonal antibody in mice. J Exp Med 178:1103–1107
18. Green LM, Reade JL, Ware CF (1984) Rapid colorimetric assay for cell viability: application to the quantitation of cytotoxic and growth inhibitory lymphokines. J Immunol Methods 70:257–268
19. van Erp NP, Gelderblom H, Guchelaar HJ (2009) Clinical pharmacokinetics of tyrosine kinase inhibitors. Cancer Treat Rev 35:692–706
20. Ogino A, Kitao H, Hirano S, Uchida A, Ishiai M, Kozuki T, Takigawa N, Takata M, Kiura K, Tanimoto M (2007) Emergence of epidermal growth factor receptor T790M mutation during chronic exposure to gefitinib in a non small cell lung cancer cell line. Cancer Res 67:7807–7814
21. Guillamo JS, Bouard SD, Valable S, Marteau L, Leuraud P, Marie Y, Poupon MF, Parienti JJ, Raymond E, Peschanski M (2009) Molecular mechanisms underlying effects of epidermal growth factor receptor inhibition of invasion, proliferation, and angiogenesis in experimental glioma. Clin Cancer Res 15:3697–3704
22. Riedel F, Götte K, Li M, Hörmann K, Grandis JR (2002) EGFR antisense treatment of human HNSCC cell lines down-regulates VEGF expression and endothelial cell migration. Int J Oncol 21: 11–16
23. Lipton A, Goessl C (2010) Clinical development of anti-RANKL therapies for treatment and prevention of bone metastasis. Bone 48:96–99
24. Fidler IJ, Kim SJ, Langley RR (2007) The role of the organ microenvironment in the biology and therapy of cancer metastasis. J Cell Biochem 101:927–936
25. Fidler IJ (2002) The organ microenvironment and cancer metastasis. Differentiation 70:498–505
26. Liotta LA, Kohn EC (2001) The microenvironment of the tumor-host interface. Nature 411:375–379

27. Langley RR, Fidler IJ (2007) Tumor cell-organ microenvironment interactions in the pathogenesis of cancer metastasis. Endocr Rev 28:297–321
28. Krampera M, Pasini A, Rigo A, Scupoli MT, Tecchio C, Malpeli G, Scarpa A, Dazzi F, Pizzolo G, Vinante F (2005) HB-EGF/HER-1 signaling in bone marrow mesenchymal stem cells: inducing cell expansion and reversibly preventing multilineage differentiation multilineage differentiation. Blood 106:59–66
29. Kim SM, Jung JU, Ryu JS, Jin JW, Yang HJ, Ko K, You HK, Jung KY, Choo YK (2008) Effects of gangliosides on the differentiation of human mesenchymal stem cells into osteoblasts by modulating epidermal growth factor receptors. Biochem Biophys Res Commun 371:866–871
30. Chien HH, Lin WL, Cho MI (2000) Down-regulation of osteoblastic cell differentiation by epidermal growth factor receptor. Calcif Tissue Int 67:141–150
31. Qin L, Tamasi J, Raggatt L, Li X, Feyen JH, Lee DC, Dicicco-Bloom E, Partridge NC (2005) Amphiregulin is a novel growth factor involved in normal bone development and in the cellular response to parathyroid hormone stimulation. J Biol Chem 280:3974–3981
32. Schneider MR, Sibilia M, Erben RG (2009) The EGFR network in bone biology and pathology. Trends Endocrinol Metab 20: 517–524
33. Furugaki K, Moriya Y, Iwai T, Yorozu K, Yanagisawa M, Kondoh K, Fujimoto-Ohuchi K, Mori K (2011) Erlotinib inhibits osteolytic bone invasion of human non-small-cell lung cancer cell line NCI-H292. Clin Exp Metastasis 28:649–659
34. Schwaninger R, Rentsch CA, Wetterwald A, van der Horst G, van Bezooijen RL, van der Pluijm G, Lowik CW, Ackermann K, Pyerin W, Hamdy FC, Thalmann GN, Cecchini MG (2007) Lack of noggin expression by cancer cells is a determinant of the osteoblast response in bone metastases. Am J Pathol 170:160–175
35. Wen YH, Koeppen H, Garcia R, Chiriboga L, Tarlow BD, Peters BA, Eigenbrot C, Yee H, Steiner G, Greco MA (2007) Epidermal growth factor receptor in osteosarcoma: expression and mutational analysis. Hum Pathol 38:1184–1191
36. Dobashi Y, Suzuki S, Sugawara H, Ooi A (2007) Involvement of epidermal growth factor receptor and downstream molecules in bone and soft tissue tumors. Hum Pathol 38:914–925
37. Di Lorenzo G, Tortora G, D'Armiento FP, De Rosa G, Staibano S, Autorino R, D'Armiento M, De Laurentiis M, De Placido S, Catalano G, Bianco AR, Ciardiello F (2002) Expression of epidermal growth factor receptor correlates with disease relapse and progression to androgen-independence in human prostate cancer. Clin Cancer Res 8:3438–3444
38. Kim SJ, Uehara H, Karashima T, Shepherd DL, Killion JJ, Fidler IJ (2003) Blockade of epidermal growth factor receptor signaling in tumor cells and tumor-associated endothelial cells for therapy of androgen-independent human prostate cancer growing in the bone of nude mice. Clin Cancer Res 9:1200–1210
39. Dunsmore SE, Rubin JS, Kovacs SO, Chedid M, Parks WC, Welgus HG (1996) Mechanisms of hepatocyte growth factor stimulation of keratinocyte metalloproteinase production. J Biol Chem 271:24576–24582
40. Yano S, Wang W, Li Q, Matsumoto K, Sakurama H, Nakamura T, Ogino H, Kakiuchi S, Hanibuchi M, Nishioka Y, Uehara H, Mitsudomi T et al (2008) Hepatocyte growth factor induces gefitinib resistance of lung adenocarcinoma with epidermal growth factor receptor-activating mutations. Cancer Res 68:9479–9487
41. Huang Y, Song N, Yanping Ding Y, Yuan S, Li X, Cai H, Shi H, Luo Y (2009) Pulmonary vascular destabilization in the premetastatic phase facilitates lung metastasis. Cancer Res 69:7529–7537
42. Baker CH, Keder D, McCarty MF, Tsan R, Weber KL, Bucana CD, Fidler IJ (2002) Blockade of epidermal growth factor receptor signaling on tumor cells and tumor-associated endothelial cells for therapy of human carcinomas. Am J Pathol 161:929–938

総　論

がん分子標的治療

曽根三郎[1,2]　倉本卓哉[2]　佐藤正大[1]　三橋惇志[1]
柿内聡司[2]　後東久嗣[1]　多田浩也[1]　西岡安彦[1]

Molecular targeted therapy for cancer

[1,2]Saburo Sone, [2]Takuya Kuramoto, [1]Seidai Sato, [1]Atsushi Mitsuhashi,
[2]Souji Kakiuchi, [1]Hisatsugu Goto, [1]Hiroya Tada, [1]Yasuhiko Nishioka
[1]Department of Respiratory Medicine and Rheumatology,
[2]Department of Medical Oncology,
Institute of Health Biosciences, The University of Tokushima Graduate School

Abstract

Recent insights into the molecular mechanism of cancer progression have given rise to specific target-directed therapies, including monoclonal antibodies and small molecular compounds, and the advent of target-specific therapeutics has remarkably improved the outcomes of patients with various malignancies. Recent advance also lead to the identification of prognostic biomarkers as predictive factors in determining response to molecular targeted drugs. Future studies also need to develop biomarkers to further increase the power of patient selection for molecular targeted therapy. Here we review the recent progress in developing new molecular targeted drugs and the resistance to treatments as well as the importance of measuring the QOL by patient-reported outcome, for personalized therapy.

Key words: cancer, molecular target, biomarker, QOL, personalized therapy

はじめに

がんは急性疾患というより，10年，20年をかけてゆっくり増殖し遠隔臓器へと転移する慢性疾患と考えられる．現在，がん治癒を期待できる治療法は，早期発見による手術切除と放射線療法のみであるが，多くのがんは診断時に所属リンパ節か周辺の組織や遠隔臓器へ微小転移を起こしているためにがん薬物療法が主体となっている．したがって，進行するがんに対する治療法としては抗がん剤による細胞毒性効果を期待するだけでなく，がんの浸潤・転移の分子機構に着目し，がん細胞の増殖・進展にかかわる重要な分子を標的とした治療，すわなち分子標的治療薬の開発が本来求められるアプローチであったが，2000年を境に大きな進展がみられている(**図1**)．その結果，ある種のがんではがん分子標的治療により長期生存が可能となっており，バイオマーカーを併用することにより効果予測が可能となり，個別化医療の時代へ前進している．一方で，がん分子標的治療は腫瘍縮小効果だけでなく，長期間にわたってQOL

[1]徳島大学大学院 呼吸器・膠原病内科　[2]同 腫瘍内科

0047-1852/10/¥40/頁/JCOPY

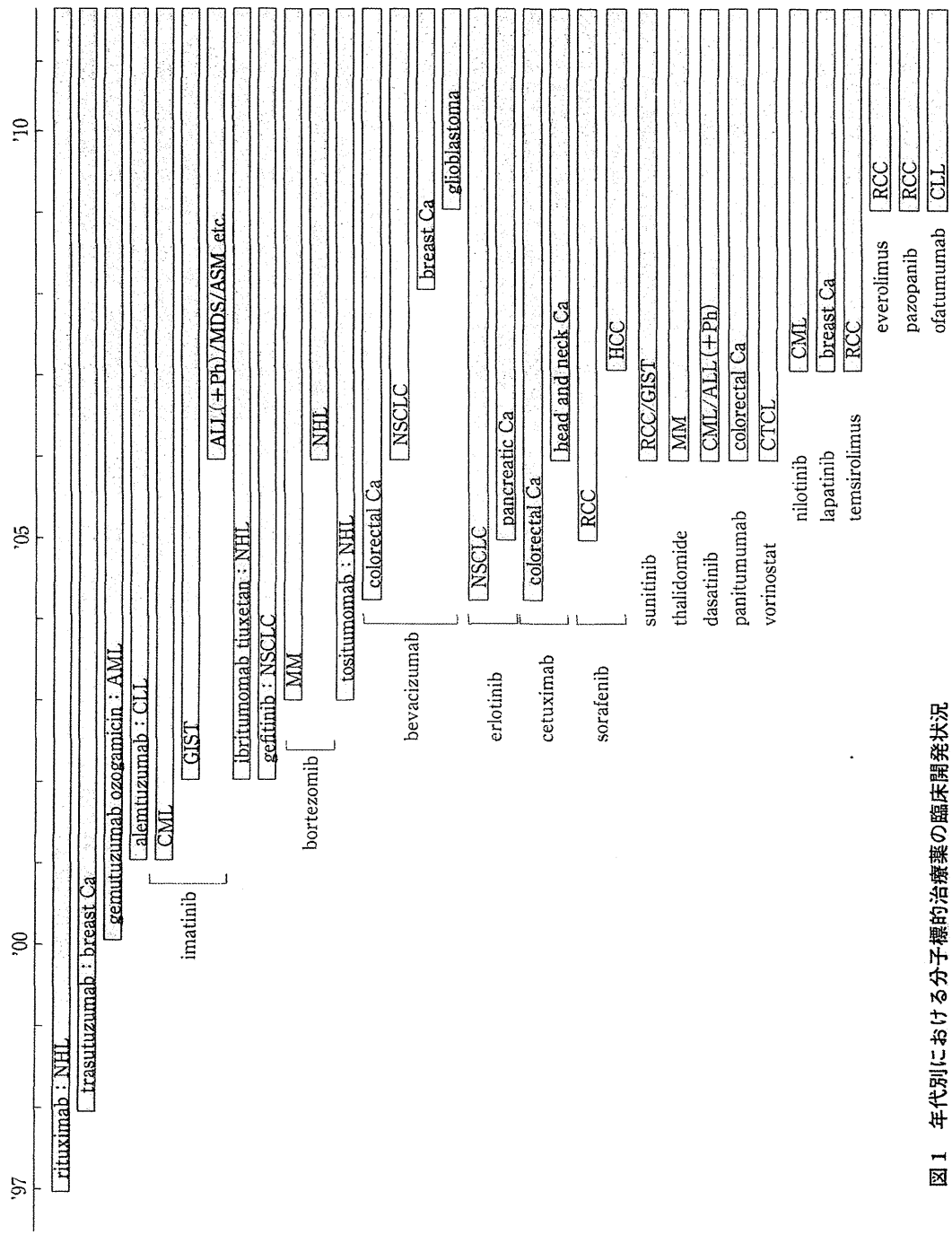

図1 年代別における分子標的治療薬の臨床開発状況
Ca: cancer.

表1 分子標的治療薬の標的分子

分類	標的分子
血管新生	血管内皮細胞増殖因子(VEGF), VEGF受容体(VEGFR), 血小板由来増殖因子(PDGF), 線維芽細胞増殖因子(FGF), IL-8
リガンド(増殖因子など)	上皮成長因子(EGF), インスリン様増殖因子-1(IGF-1), 肝細胞増殖因子(HGF), TGF, PTHrP
増殖因子受容体	EGF受容体(EGFR), IGF-1受容体(IGF-1R), PDGF受容体(PDGFR), HGF受容体(c-MET), 幹細胞因子(SCF)受容体(c-Kit), FGF受容体(FGFR), endothelin A受容体(ET1R)
細胞内情報伝達系	Bcr-Abl, JAK, SRC, RAS, MEK, RAF, PI3K, Akt, JAK2, LYN, mTOR, SYK, EML4-ALK, BRAF, MAPK, FAK, CDK, MDM2
細胞表面分子	CD20, CD22, CD25, CD52, CD56, CD40, CXCR4, MUC18
プロテアソーム	プロテアソーム, HSP90
クロマチン・DNA修飾	ヒストン脱アセチル化酵素(HDAC)

を保持できる可能性も示唆されている.

本稿では, がん分子標的治療を取り巻く最近の動向について概説したい.

1. がん転移メカニズムと標的分子

がん転移は, ①原発巣でのがん細胞増殖および血管新生, ②浸潤および脈管内への浸入, ③血流中での生存, ④標的臓器への着床, ⑤血管外への遊走, ⑥標的臓器での増殖と血管新生, という多段階反応からなり, これらすべてのステップをクリアする能力をもったごく一部のがん細胞により形成されるユニークな病態である. 浸潤・転移の各ステップにはがん細胞と宿主側の様々な正常細胞や因子との相互作用にて調節されており, 多くの分子が介在している[1,2]. それらの分子はがん治療の観点から格好の標的となっている. それらを大きく分類すると, ①主にがん細胞自身に発現される異常分子群(細胞増殖因子やそのレセプター, シグナル伝達分子, 細胞周期関連分子)と, ②宿主側の正常細胞に発現され, がん進展にかかわる分子群(血管新生関連分子, 浸潤関連分子)に分類され, それらは相互に作用する(表1). それらを分子標的とした治療薬(molecular targeted drugs)が欧米を中心に数多く臨床開発されている[3-11].

2. 腫瘍血管新生と分子標的

がん進展にかかわる生体側の正常細胞として, 腫瘍内に新生される栄養血管が古くから注目されてきた. 事実, 腫瘍内の血管密度は重要な予後因子であり, 腫瘍径が1-2mm以上と増大していくには酸素や栄養を運ぶ血管の新生が必須である. 血管新生にかかわる因子として, vascular endothelial growth factor(VEGF), basic fibroblast growth factor(bFGF), interleukin-8(IL-8), angiopoietin(Ang), matrix metalloproteinase(MMP), thymidine phosphorylase(TP)などが知られている. これらはがん細胞自身だけでなくマクロファージなど宿主側の正常細胞からも産生される. 現在, Avastin®はVEGFを標的とした抗体医薬品[11]として広く使われているが, 種々の血管新生因子(VEGF, PDGF, FGFなど)が結合する受容体の細胞内ドメインにあるチロシンキナーゼを, 単独あるいは複数阻害するものも医薬品開発され[5], 幅広いがん腫に対する臨床効果が認められている. しかし, 血管新生阻害剤の単剤治療では耐性化誘導が報告されており, そのメカニズムの解明に大きな関心が寄せられている[12].

表2-a 代表的ながん分子標的薬開発(第I相試験)

project name	target	開発段階	project name	target	開発段階
GSK-690693	Akt1, 2, 3	PI	XL-019	JAK2	PI
R-547	CDK1, 2, 4	PI	CH-4987655	MAPK	PI
AMG-208	c-MET	PI	RG-7112	MDM2	PI
E-7050	c-MET, VEGFR2	PI	AZD-2014	mTOR	PI
NVP-AEE-788	EGFR, HER2, VEGFR	PI	GDC-0980	PI3K	PI
PF-04554878	FAK	PI	RG-4733	γ-secretase	PI
JNJ-26481585	HDAC	PI	CP-870893	CD40 agonist	PI
KW-2478	HSP90	PI	MDX-1338	CXCR4	PI
KW-2450	IGF-1R	PI	RG-7414	EGF-like domain 7	PI
BAY-36-1677	IL-4 agonist	PI	ABX-MA1	MUC18	PI

表2-b 代表的な抗体医薬品開発(第II相から承認医薬品)

種 類	一般名	商品名/project name	target	開発段階	適応/治験実施がん腫
抗体医薬品	bevacizumab	Avastin®	VEGF	承認済み	転移性大腸癌, 肺癌, 乳癌
	cetuximab	Erbitax®	EGFR	承認済み	転移性大腸癌, 頭頸部癌, 肺癌
	panitumumab	Vectibix	EGFR	承認済み	転移性大腸癌
	rituximab	Rituxan®	CD20	承認済み	リンパ腫(CD20陽性B細胞性)
	trastuzumab	Herceptin®	HER2	承認済み	乳癌(HER2陽性)
	denosumab	AMG162	RANKL	PIII	進行乳癌患者の骨転移
	pertuzumab	R1273	二量体化HER2	PIII	乳癌など
	figitumumab	CP-751, 871	IGF-1R	PIII	NSCLCなど
	mapatumumab	HGS1012	TRAIL-R1	PII	NSCLC, 肝細胞癌など
	nimotuzumab	DE-766	EGFR	PIII	胃癌, 大腸癌, NSCLC, HNSCCなど

3. がん分子標的薬の特徴と分類

既存の抗がん剤は殺細胞活性によりスクリーニングされ, 有害事象として骨髄抑制, 悪心・嘔吐が多いが, がん分子標的薬は, がん進展にかかわる標的分子の阻害活性によりスクリーニングし, 多くは有害事象としての骨髄抑制, 悪心・嘔吐が少ない点が特徴的である. 最近では米国FDAで承認されるがん治療薬の7, 8割が分子標的治療薬と報告されている. 現在, 医薬品として承認されている代表的な分子標的薬ならびに臨床開発中の候補薬を**表2**に示したが, 現在, 前臨床試験中のものを入れると100以上あると思われる.

がん治療のための分子標的薬は, 抗がん剤とは全くコンセプトの異なる抗体医薬品と小分子阻害剤と大きく作用面から2つに分類され, それぞれ利点をもっている.

a. 抗体医薬品

抗体医薬品はがん細胞膜上に発現している分子(受容体など)や受容体のリガンドなどに特異的に結合する抗体を遺伝子操作にてヒト型化したものが多く, 注射薬として使われる. 代表的な抗体医薬品の標的分子として, VEGF, EGF受容体, CD20, HER2などがあげられる(**表2-b**). 最近, IGF-1受容体に対する抗体薬が注目されている. それらの作用機序は, リガンドのレセプターへの結合阻害と, ADCC(抗体依存

表2-c 代表的な小分子阻害剤開発(第II相から承認医薬品)

種類	一般名	商品名/project name	開発段階	target	適応/治験実施がん腫
小分子阻害剤	bortezomib	VELCADE®	承認済み	proteasome	再発多発性骨髄腫
	dasatinib	Sprycel®	承認済み	Bcr-Abl	慢性骨髄性白血病(イマチニブ抵抗性)・ALL
	erlotinib	Tarceva®	承認済み	EGFR	肺癌(再発非小細胞性)
	gefitinib	Iressa®	承認済み	EGFR	肺癌(再発非小細胞性)
	imatinib	Gleevec®	承認済み	PDGFR	慢性骨髄性白血病(Ph1陽性)
	lapatinib	Tykerb®	承認済み	EGFR, HER2	転移性乳癌
	nilotinib	Tasigna®	承認済み	Bcr-Abl	慢性骨髄性白血病(イマチニブ抵抗性)
	sorafenib	Nexavar®	承認済み	VEGFR1, 2, 3, FGFR1, PDGFRβ, BRAF	転移性腎癌, 肝細胞
	sunitinib	Sutent®	承認済み	VEGFR1, 2, 3, FGFR1, PDGFRβ	転移性腎癌, 肝細胞, GIST
	temsirolimus	Torisel®	承認済み	mTOR	転移性腎癌
	olaparib	AZD2281	PII	PARP	乳癌など
	motesanib diphosphate	AMG-706	PIII	VEGFR, PDGFR, c-Kit	NSCLCなど
	enzastaurin	LY-317615	PIII	PKCβ, Akt	グリオーマなど
	zibotentan	ZD-4054	PIII	ETAR	前立腺癌など
	cediranib	AZD-2171	PIII	VEGFR	NSCLCなど
	linifanib	ABT-869	PIII	VEGFR, PDGFR	大腸癌, 乳癌, 肝細胞癌, NSCLC, 転移性腎癌など
		E-7080	PII	VEGFR, FGFR, c-Kit, RET	肝細胞癌, 甲状腺癌など
		TSU-68	PII	VEGFR, FGFR, PDGFRβ	乳癌, 肝細胞癌など
		YM-155	PII	survivin	メラノーマ, DLBCL, 前立腺癌, 乳癌(HER2陰性), NSCLCなど
	saracatinib	AZD-0530	PII	Src, Abl	卵巣癌, 乳癌, 膵癌, 胃癌, 大腸癌, 頭頸部癌など
		BMS-754807	PII	IGF-1R	乳癌など
		RO-5185426	PIII	BRAF	メラノーマなど
	selumetinib	AZD-6244	PII	MEK	NSCLC, メラノーマ, 肝癌など
		ARQ-197	PII	c-MET	NSCLC, RCC, 膵癌など
	foretinib	XL-880	PII	c-MET, VEGFR, PDGFR	頭頸部癌など
	vismodegib	GDC-0449	PII	hedgehog	卵巣癌, 大腸癌など